

High-Dimensional Chaotic Attractors in a Gyrotron with Nonstationary Field Structure

E. V. Blokhina*, S. P. Kuznetsov, and A. G. Rozhnev

Saratov State University, Saratov, Russia

* e-mail: BlokhinaEV@yandex.ru

Received December 5, 2005

Abstract—The chaotic dynamics of a gyrotron with nonstationary field structure has been numerically simulated and the Lyapunov exponents of chaotic attractors are calculated. The dimensions of chaotic attractors estimated using the Kaplan–Yorke formula have proved to be anomalously high. This fact is related to the presence of a large number of high- Q eigenmodes in the gyrotron resonator operating in the vicinity of a critical frequency of the slow-wave system.

PACS numbers: 84.40.Ik

DOI: 10.1134/S1063785006040274

One of the main properties of dynamic chaos is the exponential instability of phase trajectories [1–3]. This instability can be quantitatively characterized in terms of the Lyapunov exponents calculated for attractors of a given system. In the case of a system with N -dimensional phase space, there is a spectrum of N such exponents wherein positive and negative values refer to the exponential growth and decay of perturbations near the typical trajectories belonging to the given attractor. Chaotic attractors are characterized by the presence of at least one positive Lyapunov exponent in this spectrum.

Analysis of the spectrum of Lyapunov exponents is widely used for the investigation of complicated dynamics both in systems described by ordinary differential equations and in models (maps) with discrete time. In recent years, the ideas and methods of nonlinear dynamics have been extensively used for the investigation of distributed systems of the electron-wave nature such as backward-wave oscillators (BWOs), gyrotrons, and delayed feedback oscillators based on traveling-wave tubes (TWTs) and klystrons. Now it is reliably established that, for certain sets of parameters, these systems can feature single-mode, multimode, and chaotic oscillations. For the investigation of dynamics and the illustrative representation of results, it is convenient to use time series, spectra, phase portraits, and bifurcation diagrams. We believe that an analysis of the spectrum of Lyapunov exponents will provide a deeper insight into the nature of regimes observed in such systems.

Since the systems under consideration are distributed (i.e., possess infinite dimension), the number of Lyapunov exponents in the spectrum has to be also infinitely large. However, only a limited subset of this infinite set is important in practice. This subset represents a sequence of decreasing exponents whose number is

sufficient for determining the dimension (so-called Lyapunov dimension) of the corresponding attractor using the well-known Kaplan–Yorke formula [1–3].

To the present, several papers have been published in which the Lyapunov exponents have been used for the characterization of nonlinear dynamics of electron-wave devices. The first investigation of this kind was reported in [4], where chaotic oscillations in a BWO were considered and the corresponding major Lyapunov exponent was estimated. The results of numerical simulations and experiments showed that chaos in this electron-wave system is related to the instability of its dynamics with respect to small perturbations in the initial conditions. Recently, several Lyapunov exponents were calculated for a BWO model [5] and the dimensions of attractors corresponding to chaotic regimes in this system were estimated. It was established that, depending on the electron beam current, the system can feature chaotic regimes either with a single positive exponent (weak chaos) or with several positive exponents (developed chaos or hyperchaos). Dronov et al. [5] considered chaotic dynamics in a TWT and obtained estimates for several Lyapunov exponents.

The nonlinear dynamics of a gyrotron with nonstationary longitudinal field structure was originally studied by Ginzburg et al. [7]. Based on the numerical solution of equations describing this dynamics, it was established that automodulation regimes are possible in this system. Later, Airila et al. [8] modeled nonstationary oscillatory processes in a gyrotron in a broad range of parameters. Recently, automodulation regimes were experimentally realized in gyrotrons with delayed feedback (see, e.g., [9, 10]). The results of our recent numerical simulations [11] showed that the transition to chaos can proceed according to various scenarios,

either via a cascade of period-doubling bifurcations or via breakage of quasi-periodic motion regimes.

Below, we present and discuss the results of calculations of the spectrum of Lyapunov exponents for chaotic regimes in a gyrotron with nonstationary longitudinal field structure. The Lyapunov dimensions of the attractors for these regimes will be estimated using the Kaplan–Yorke formula. In contrast to electron-wave systems of the BWO type, a gyrotron operating in the vicinity of a critical frequency of the slow-wave system is characterized by a large number of Lyapunov exponents with small absolute values. This fact is related to the large number of high- Q eigenmodes of the slow-wave system and leads to a rather unexpected conclusion concerning very high dimensions of chaotic attractors. These dimensions are much greater than those of chaotic attractors in the other electron-wave systems studied so far.

The dynamics of a gyrotron with nonstationary longitudinal field structure will be considered on the basis of a numerical solution of the following system of equations written in terms of the dimensionless variables and parameters:

$$\frac{\partial^2 F}{\partial x^2} - i \frac{\partial F}{\partial t} = \frac{I_0}{2\pi} \int_0^{2\pi} p(\varphi) d\varphi_0, \quad (1)$$

$$\frac{dp}{dx} + ip(|p|^2 + \Delta - 1) = iF, \quad p|_{x=0} = e^{i\varphi_0}, \quad \varphi_0 \in [0, 2\pi].$$

Here, $F(x, t)$ is a function describing the instantaneous longitudinal distribution of the complex amplitude of the high-frequency field, p is the transverse momentum of electron, Δ is the mismatch between the cyclotron frequency and the critical frequency of the working waveguide mode, and I_0 is the electron beam current. The interaction equations are supplemented by the following initial condition for the field: $F(x, 0) = F_0(x)$.

Let the boundary condition at the entrance cross section correspond to the total reflection, whereby the field is always zero: $F(0, t) = 0$. At the collector end (exit cross section), the gyrotron is loaded on a horn antenna with a small opening angle. An adequate form of the boundary condition for this case was established in [12]. According to this, the absolute value of the reflection coefficient smoothly decreases with increasing frequency (see curve *A* in the inset to Fig. 1). An alternative variant for a gyrotron with the typical resonator geometry is offered by approximate boundary conditions, whereby the absolute value of the reflection coefficient depends on the frequency as described by curve *B* in the same inset to Fig. 1.¹

¹ In what follows, the boundary conditions for a horn antenna with the frequency dependence of the reflection coefficient corresponding to curves *A* and *B* in Fig. 1 will be referred to as the boundary conditions of types *A* and *B*, respectively.

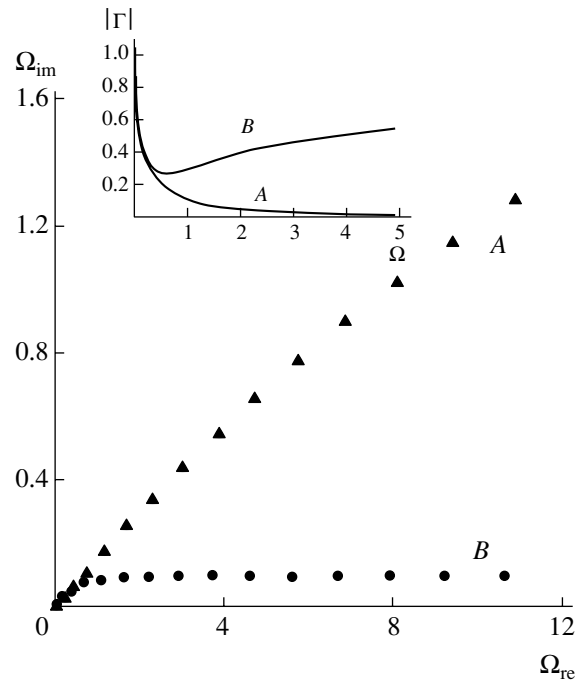


Fig. 1. Frequencies of the linear modes of a “cold” system on the complex plane (Ω_{re} , Ω_{im}) for the boundary conditions of types *A* (curve *A*) and *B* (curve *B*) in the exit plane of the waveguide. The inset shows plots of the absolute value of the reflection coefficient versus frequency for boundary conditions of the corresponding types.

The map of gyrotron regimes on the plane of the main parameters (Δ , I_0), which was obtained in [11], contains regions corresponding to various types of generation (stationary, automodulation, chaos). It was established that, in addition to a chaotic regime characterized by a single positive Lyapunov exponent (“weak” chaos), the gyrotron can also feature the regimes (referred to as the developed chaos or hyperchaos) with several positive Lyapunov exponents [13].

Figures 2a–2c present plots illustrating the regime of hyperchaos, which corresponds to a numerical solution of Eqs. (1) with the boundary conditions of type *B*. The first diagram (Fig. 2a) shows the time series of the electron efficiency $\eta(t)$ that is calculated using the transverse momentum of electrons at the collector end of the system. Figure 2b shows a phase portrait constructed using the values of $\eta(t)$ at the current time and at the delayed moment. Figure 2c presents the spectrum determined using the Fourier analysis of the complex amplitude of a signal at the gyrotron output. In contrast to the case of weak chaos, the regime of hyperchaos has (i) a continuous spectrum that is more homogeneous with respect to the power distribution and (ii) a phase portrait that is characterized by the absence of any pronounced structure.

In order to calculate the spectrum of Lyapunov exponents, we have used the Benettin algorithm [1–3] adapted to a distributed electron-wave system as

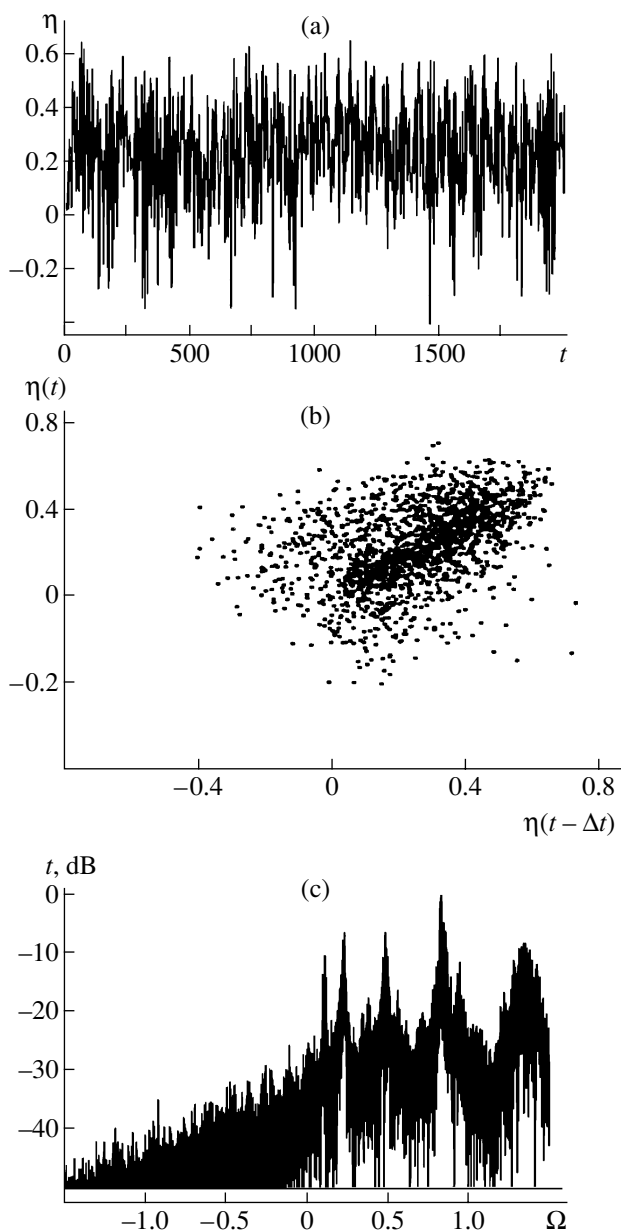


Fig. 2. Plots illustrating the regime of hyperchaos in a gyrotron described by Eqs. (1) with $\Delta = 1.0$, $I_0 = 0.15$ and output boundary conditions of type *B*: (a) a typical time series of the electron efficiency $\eta_{\perp} = 1 - 1/(2\pi) \int_0^{2\pi} |p|^2 d\phi_0$; (b) the phase portrait reconstructed from this time series; (c) the field spectrum at the gyrotron output.

described in [5]. The set of N exponents is obtained from a numerical solution of $N + 1$ sets of Eqs. (1) with boundary conditions of the *A* and *B* types, in which the initial conditions for the field are set by close complex functions $F_n(x) = F(x) + \epsilon \tilde{F}_n(x)$, where $\tilde{F}_n(x)$ has a norm of unity and ϵ is a small quantity. After each time step $\Delta\tau$, the solution perturbations are orthogonalized and normalized using the Gram–Schmidt algorithm. Then, N values of S_n are calculated at each step, which

represent the accumulating sums that show a change in the norm of n th perturbation upon M steps of the algorithm. Using these sums, the Lyapunov exponents Λ_n are estimated as follows:

$$S_n = \sum_{i=1}^M \ln \|\tilde{F}_n(t = i\Delta\tau)\|, \quad \Lambda_n = S_n/M\Delta\tau. \quad (2)$$

In order to obtain a more precise estimate, the time variation of the accumulating sum (2) is approximated by a straight line using least squares, and then Λ_n is determined as the slope of this line.

Once a sufficiently large number of Lyapunov exponents are determined, the Lyapunov dimension of the attractor can be determined using the Kaplan–Yorke formula [3]:

$$D = m + \frac{\sum_{i=1}^m \Lambda_i}{|\Lambda_{m+1}|}, \quad (3)$$

where m is a number such that $\sigma_m = \sum_{i=1}^m \Lambda_i > 0$,

whereas $\sigma_{m+1} = \sum_{i=1}^{m+1} \Lambda_i < 0$. As is known from numerous examples considered in the literature on non-linear dynamics, the value given by formula (3) usually provides a good estimate of the fractal dimension for a chaotic attractor.

Using the procedure described above, we have calculated the Lyapunov exponents for several regimes of weak and developed chaos in a gyrotron described by Eqs. (1) with boundary conditions of the *A* and *B* types. Figure 3a shows the plots of several accumulating sums σ_n obtained in the course of calculations of the spectrum of Lyapunov exponents in a regime of hyperchaos. The values of $S_n(t)$ monotonically increasing on the average correspond to positive exponents. It should be noted that attractors of the given system, which correspond to the automodulation and chaotic regimes, possess at least two zero exponents (for which perturbations corresponding to a shift of the solution with respect to phase and time neither increase nor decrease with the time).

Figure 3b shows plots of the accumulating sums σ_n for the first Lyapunov exponents (enumerated in the order of decrease) versus the number n of terms in the sum. Here, curves 1 and 2 correspond to weak chaos regimes with $\Delta = 0.0$, $I_0 = 0.0365$ (boundary conditions *A*) and $\Delta = 0.0$, $I_0 = 0.038$ (boundary conditions *B*), respectively. Curves 3 and 4 correspond to developed chaos regimes with $\Delta = 1.0$, $I_0 = 0.11$ (boundary conditions *A*) and $\Delta = 1.0$, $I_0 = 0.15$ (boundary conditions *B*), respectively. The point of intersection of each curve with the abscissa axis give an estimate of the Lyapunov dimension according to the Kaplan–Yorke formula.

Let us consider the estimates of attractor dimensions for various regimes. In a system with the boundary conditions of type *A*, the attractor dimension in a regime of weak chaos is approximately $D \approx 16.4$, while that in a regime of hyperchaos is about 30.6. In the case of boundary conditions *B*, the attractor dimensions increase to $D \approx 26.6$ for weak chaos and $D \approx 40.7$ for hyperchaos. For the comparison, it should be noted that the estimates of attractor dimensions obtained for a BWO in the regimes of weak and developed chaos were 3.5 and 6.4, respectively [5]. For a TWT with delayed feedback, the chaotic attractor dimension was estimated as $2 < D < 3$ [6]. Thus, the dimensions of chaotic attractors in our system are substantially higher than those obtained for the other electron-wave systems. We believe that this difference is related to the fact that the gyrotron under consideration operates in the vicinity of a boundary of the transmission band of the slow-wave system.

In order to illustrate this explanation, let us consider the “cold” system (i.e., that in the absence of the electron beam), which corresponds to setting $I_0 = 0$ in Eqs. (1). In this case, the system has a trivial solution $F(x, t) \equiv 0$ that is evidently robust. Then, let us represent a field perturbation in the cold system as a superposition of linear eigenmodes of the distributed resonator formed by the slow-wave system, with the corresponding boundary conditions. Each mode will decay with time according to the law $\sim \exp(-\Omega_{im,n}t)$, where $\Omega_{im,n}$ is the imaginary part of the frequency for this eigenmode. The Lyapunov exponents calculated for the cold system with perturbations in the trivial solution must decay to zero as $\sim \exp(\Lambda_n t)$, so that $\Lambda_n > 0$. Thus, the cold system must obey the relation $\Lambda_n = -\Omega_{im,n}$. The values of imaginary parts of the eigenmode frequencies calculated using Eqs. (1) with the boundary conditions *B* are presented in the table in comparison to the estimates of Lyapunov exponents for a cold system obtained for the trivial solution using the proposed numerical algorithm. As can be seen the two values are in quite good agreement.

Figure 1 shows the linear eigenmode frequencies for a cold system on the complex plane (curves *A* and *B* refer to the values calculated for the boundary conditions of types *A* and *B*, respectively). An analysis of the complex frequencies of linear eigenmodes leads to a conclusion that the slow-wave system features a large number of modes with relatively high Q (with a small positive imaginary part), which are weakly coupled to the electron beam. For boundary conditions of the *B* type, the decay times of such modes are on the same (sufficiently large) order of magnitude. Then, the relaxation time of a small random perturbation arising on the background of the fundamental modes and containing the aforementioned high- Q modes will coincide in the order of magnitude with their characteristic decay time. Therefore, a large number of negative Lyapunov exponents with small absolute values will be also contained

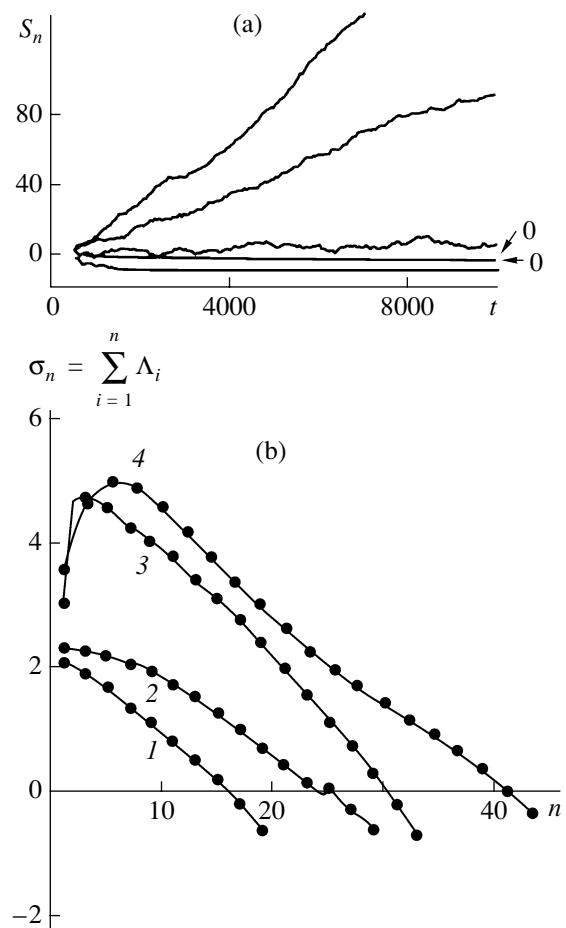


Fig. 3. Plots of the accumulating sums σ_n (a) versus time t in the regime of hyperchaos with $\Delta = 1.0$, $I_0 = 0.15$ and (b) versus the number of terms in the sum for (1, 2) weak chaos regimes with $\Delta = 0.0$, $I_0 = 0.0365$ (boundary conditions *A*) and $\Delta = 0.0$, $I_0 = 0.038$ (boundary conditions *B*), respectively, and (3, 4) developed chaos regimes with $\Delta = 1.0$, $I_0 = 0.11$ (boundary conditions *A*) and $\Delta = 1.0$, $I_0 = 0.15$ (boundary conditions *B*), respectively.

in the spectrum of a system in the presence of the electron beam. Depending on the type of the boundary conditions, the system of such “cold” eigenmodes may contain either relatively high- Q (for boundary conditions of the *B* type) or low- Q (for the boundary conditions *A*), and the difference of imaginary parts of the frequencies of higher eigenmodes can be rather significant (see Fig. 1). For this reason, the estimates of the attractor dimension obtained for the system with boundary conditions of the *A* type are significantly lower than those in the case of boundary conditions *B*.

In conclusion, we have numerically calculated the Lyapunov exponents for chaotic regimes in a gyrotron with nonstationary field structure and estimated the attractor dimensions for the regimes of weak and developed chaos in this system. The results showed anomalously high values of the attractor dimension in com-

Table

1	$-\Omega_{im}$	n	Λ
1	-0.00685	1	-0.0094
2	-0.0259	2	-0.0263
3	-0.05123	3	-0.0522
4	-0.07238	4	-0.0623
5	-0.08451	5	-0.0650
6	-0.09024	6	-0.0801
7	-0.09295	7	-0.0891
8	-0.09431	8	-0.0923
9	-0.09506	9	-0.0984
10	-0.09551	10	-0.0989

parison to those reported for the other electron-wave systems. This phenomenon is explained by the presence of a large number of high- Q eigenmodes weakly interacting with the electron beam in the gyrotron resonator operating in the vicinity of a critical frequency of the slow-wave system.

REFERENCES

1. H. G. Schuster, *Deterministic Chaos* (Physik-Verlag, Weinheim, 1984).

2. E. Ott, *Chaos in Dynamical Systems* (Cambridge Univ. Press, New York, 1993).
3. S. P. Kuznetsov, *Dynamic Chaos* (Fizmatlit, Moscow, 2001) [in Russian].
4. B. P. Bezruchko, L. V. Bulgakova, S. P. Kuznetsov, and D. I. Trubetskov, *Radiotekh. Élektron. (Moscow)* **28**, 1136 (1983).
5. S. P. Kuznetsov and D. I. Trubetskov, *Izv. Vyssh. Uchebn. Zaved., Radiofiz.* **47** (5), 1 (2004).
6. V. Dronov, M. R. Hendry, T. M. Antonsen, and E. Ott, *Chaos* **14**, 30 (2004).
7. N. S. Ginzburg, N. A. Zavolskii, G. S. Nusinovich, and A. S. Sergeev, *Izv. Vyssh. Uchebn. Zaved., Radiofiz.* **29** (1), 106 (1986).
8. M. i. Airila, O. Dumbrajs, A. Reinfelds, and U. Strautins, *Phys. Plasmas* **8**, 4608 (2001).
9. N. S. Ginzburg, N. I. Zaitsev, E. V. Ilyakov, et al., *Pis'ma Zh. Tekh. Fiz.* **28** (9), 85 (2002) [*Tech. Phys. Lett.* **28**, 395 (2002)].
10. R. M. Rozental, N. I. Zaitsev, I. S. Kulagin, et al., *IEEE Trans. Plasma Sci.* **32**, 418 (2004).
11. E. V. Blokhina and A. G. Rozhnev, *Radiotekh. Élektron. (Moscow)* **49**, 1390 (2004).
12. A. G. Rozhnev, *J. Commun. Technol. Electron.* **45**, 595 (2000).
13. E. V. Blokhina and A. G. Rozhnev, in *Proceedings of the 6th International Vacuum Electronics Conference (IVEC), Noordwijk (Netherlands), 2005*, pp. 133–134.

Translated by P. Pozdeev